An Electrochemical Study of the Oxidation of Hydrogen at Platinum Electrodes in Several Room Temperature Ionic Liquids †

ARTICLE *in* THE JOURNAL OF PHYSICAL CHEMISTRY B · MAY 2007

Impact Factor: 3.3 · DOI: 10.1021/jp067236v · Source: PubMed

4 AUTHORS, INCLUDING:

Debbie S. Silvester
Curtin University
55 PUBLICATIONS **1,684** CITATIONS
SEE PROFILE

Leigh Aldous
University of New South Wales
89 PUBLICATIONS **1,836** CITATIONS
SEE PROFILE

An Electrochemical Study of the Oxidation of Hydrogen at Platinum Electrodes in Several Room Temperature Ionic Liquids†

Debbie S. Silvester,‡ Leigh Aldous,§ Christopher Hardacre,§ and Richard G. Compton*,‡

Physical and Theoretical Chemistry Laboratory, Oxford University, South Parks Road, Oxford OX1 3QZ, United Kingdom, School of Chemistry and Chemical Engineering/QUILL, Queen's University Belfast, Belfast, Northern Ireland BT9 5AG, United Kingdom

Received: November 2, 2006; In Final Form: January 7, 2007

The electrochemical oxidation of dissolved hydrogen gas has been studied in a range of room-temperature ionic liquids (RTILs), namely $[C_2mim][NTf_2]$, $[C_4mim][NTf_2]$, $[N_{6,2,2,2}][NTf_2]$, $[P_{14,6,6,6}][NTf_2]$, $[C_4mpyrr][NTf_2]$, $[C_4mim][BF_4]$, $[C_4mim][PF_6]$, $[C_4mim][OTf]$, and $[C_6mim]Cl$ on a platinum microdisk electrode of diameter 10 μm. In all cases, except $[C_6mim]Cl$, a broad quasi-electrochemically reversible oxidation peak between 0.3 to 1.3 V vs Ag was seen prior to electrode activation ($[C_6mim]Cl$ showed an almost irreversible wave). When the electrode was pre-anodized ("activated") at 2.0 V vs Ag for 1 min, the peak separations became smaller, and the peak shape became more electrochemically reversible. It is thought that the electrogenerated protons chemically combine with the anions (A^-) of the RTIL. The appearance and position of the reverse (reduction) peak on the voltammograms is thought to depend on three factors: (1) the stability of the protonated anion, HA, (2) the position of equilibrium of the protonation reaction $HA \rightleftharpoons H^+ + A^-$, and (3) any follow-up chemistry, e.g., dissociation or reaction of the protonated anion, HA. This is discussed for the five different anions studied. The reduction of $HNTf_2$ was also studied in two $[NTf_2]^-$-based RTILs and was compared to the oxidation waves from hydrogen. The results have implications for the defining of pK_a in RTIL media, for the development of suitable reference electrodes for use in RTILs, and in the possible amperometric sensing of H_2 gas.

1. Introduction

Room-temperature ionic liquids (RTILs) have attracted much attention recently in many areas of science, particularly in green synthesis,[1,2] mainly due to their nonvolatility and interesting physical characteristics. They have been used in many electrochemical applications such as solar cells,[3] electrochemical sensors,[4] fuel cells,[5] capacitors,[6] and in lithium batteries[7] and are employed as solvents in electrochemical experiments[8,9] because they are intrinsically conductive (no need for supporting electrolyte). Also, they have wide electrochemical windows, allowing for electrodeposition[10] of metals and semiconductors normally out of the range of traditional solvents. They can also be employed as supporting electrolytes in other solvents such as acetonitrile (MeCN).[11] As part of a general understanding of electrochemistry in RTILs, we have previously looked at the mechanisms of various organic reactions,[12−16] with a view to identify any similarities or differences to the reactions in RTILs compared to conventional aprotic solvents. In general, the studies reveal that the mechanisms often appear to be similar in both media, with the main differences due to the higher viscosity of RTILs giving slower diffusion. In addition, the electrode kinetics of oxidation and reduction are often slowed in RTILs.[17−19] We have, however, shown that RTILs can offer some advantages over traditional solvents, for example, in studying the electrochemistry of the inorganic compounds PCl_3 and $POCl_3$.[20] These compounds were found to be "stable" in some RTILs[21] (but would otherwise hydrolyze in traditional molecular solvents), and the electrochemistry was studied in detail for the first time.

One of the most important applications of RTILs in electrochemistry to date is their use in gas sensors.[4,22,23] Their nonvolatility means that the sensor does not "dry out" (as with conventional aqueous solution-based Clark cells), and their high thermal stability allows gas sensing at high temperatures. A range of gases, including oxygen (O_2),[24] ammonia (NH_3),[25] and carbon dioxide (CO_2, from O_2 and CO_2 simultaneously)[26] have been studied previously in RTILs, and these solvents have shown promise for use as electrolytes in a range of industrial gas sensors.

It is of general interest to explore the oxidation of hydrogen (H_2) due to its major importance in fuel cells[27] among other applications. The oxidation of gaseous hydrogen is (at least in principle) believed to be conceptually one of the simplest processes, involving a simple one-electron transfer per proton. The electrochemical oxidation of hydrogen has been studied on platinum and palladium surfaces in protic solvents[28−31] such as H_2O, but relatively little work has been done in aprotic solvents. Barrette and Sawyer[32] showed reversible oxidation waves for dissolved H_2 in dimethyl sulfoxide (DMSO), pyridine, *N*,*N*-dimethylformamide (DMF), and acetonitrile (MeCN) and observed broad, diffuse anodic peaks whose peak currents were irreproducible and not proportional to the partial pressure of H_2. However, when the electrodes were activated electrochemically (pre-anodized) at potentials more positive than the initial peaks, the H_2 oxidation peak changes from a shape characteristic of an electrochemically quasi-reversible process to one for a nearly reversible one-electron transfer. In all solvents except

† Part of the special issue "Physical Chemistry of Ionic Liquids".

* Author to whom all correspondence should be addressed. E-mail: richard.compton@chemistry.oxford.ac.uk. Telephone: +44 (0) 1865 275 413. Fax: +44 (0) 1865 275 410.

‡ Physical and Theoretical Chemistry Laboratory.

§ School of Chemistry and Chemical Engineering/QUILL.

10.1021/jp067236v CCC: $37.00
Published on Web 02/07/2007

MeCN, reversible waves with peak currents proportional to the partial pressure of H_2 were observed, allowing, in principle, for a quantitative analysis of the solubility of H_2.

Daniele and Bontempelli[33] have also investigated the H^+/H_2 redox couple in a range of organic polar solvents. By the *in situ* electrogeneration of anhydrous perchloric acid, and assuming its subsequent quantitative dissociate in line with

$$HClO_4 + S \rightleftharpoons HS^+ + ClO_4^- \quad (1)$$

where S = solvent, the half-wave potential for the reversible H^+/H_2 system could be related to the relative bulk solvent basicity. This system was then expanded to electrochemically evaluate a range of added bases, although both cases relied upon the use of a reference system that was strictly independent of the nature of the solvent.[33]

Concerning ionic liquids, Welton and co-workers[34] have used Kamlet−Taft parametrization to investigate a range of cations and anions, which gave trends in order of their basicity and their relative hydrogen bonding accepting and donating ability. Conventional acid−base indicators have also been used to physically probe the inherent acidity and basicity of ionic liquids; however, such probes are not calibrated toward ionic liquids, and all observed color changes can be the result of hydrogen bonding interactions in addition to acid−base equilibria.[35−37] In addition, the nature of the solvation of strong acids in ionic liquids (e.g., $H_xS_y^{y+}$) has still to be conclusively demonstrated, and little is understood about the nature and relative strength of acidity within these ionic systems, despite numerous previous applications of inherently Brønsted acidic ionic liquids.[38−41] Del Popolo and co-workers[42] carried out a first principles simulation study in order to investigate the solvation structure of a proton, simulating HCl dissolved in the ionic liquid [C_1mim]Cl. Rather than dissociation, this revealed the immediate formation of the anion $[HCl_2]^-$. At its most stretched configuration, $[HCl_2]^-$ can only be considered as [Cl−HCl]$^-$, and the breaking of one H−Cl bond resulted in the formation of a new H−Cl bond, highlighting the possibility of proton transport by proton "hopping", moving from chloride to chloride.

Anomalies relating to protons in ionic liquids have also been observed in catalytic reactions. For Friedel−Craft reactions performed in ionic liquids using both Lewis- and Brønsted-based catalysts, reactions have been observed to only perform well in ionic liquids based upon the bis{(trifluoromethyl)-sulfonyl}imide anion ($[NTf_2]^-$) compared with $[OTf]^-$ and $[BF_4]^-$.[43,44] In addition, in $[NTf_2]^-$-based ionic liquids, the acid catalysts HBF_4 and HOTf demonstrate significantly lower reaction rates than $HNTf_2$, despite all three being strong acids in water.

In the present report, the oxidation of hydrogen (H_2) has been studied in a range of room-temperature ionic liquids (RTILs) incorporating different common cations and anions, namely [C_2-mim][NTf_2], [C_4mim][NTf_2], [C_4mpyrr][NTf_2], [C_4mim][BF_4], [C_4mim][PF_6], [C_4mim][OTf], and [C_6mim]Cl (for structures, see Figure 1). A main focus of this work was to ascertain if reversible oxidation waves could be obtained for the oxidation of H_2 in ionic liquid(s) where the product, HS^+, was stable (or not) on the voltammetric time scale. We anticipate the following reaction for the oxidation of hydrogen in a solvent (S):

$$H_2 - 2e^- + 2S \rightleftharpoons 2HS^+ \quad (2)$$

where the product HS^+ is either stable or unstable. If the product is stable, chemically reversible voltammetry is expected, whereas

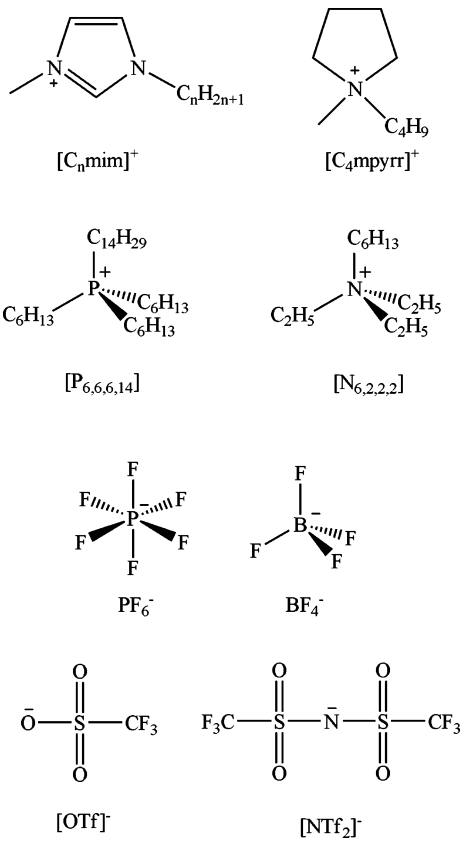

Figure 1. Molecular structures of the cations and anions employed in the RTILs in this study

if the product is unstable, a chemically irreversible voltammetric wave will be obtained. We have also studied the reduction of the acid $HNTf_2$ in two $[NTf_2]^-$-based RTILs (where HS^+ (≡ $HNTf_2$) is stable) to give an insight into the H^+/H_2 redox couple. It is believed that this process can shed light on the nature of acidic proton−ionic liquid interactions, ultimately helping to define a pK_a scale in RTIL media and to develop suitable reference electrodes for use in RTILs. This work also has implications in the possible amperometric sensing of H_2 gas.

2. Experimental

2.1. Chemical Reagents. 1-Ethyl-3-methylimidazolium bis-{(trifluoromethyl)sulfonyl}amide ([C_2mim][NTf_2]), 1-butyl-3-methylimidazolium bis{(trifluoromethyl)sulfonyl}amide ([C_4-mim][NTf_2]), and 1-butyl-1-methylpyrrolidinium bis{(trifluoromethyl)sulfonyl}amide ([C_4mpyrr][NTf_2]) and their bromide salt precursors were prepared by standard literature procedures.[45,46] 1-Hexyl-3-methylimidazolium chloride ([C_6mim]Cl) was also prepared according to previous literature methods.[45] *n*-Hexyltriethylammonium bromide (Aldrich, 99%) and tris(*n*-hexyltetradecylphosphonium chloride (Cytec) were used as purchased for metathesis with lithium bis{(trifluoromethyl)sulfonyl}amide and subsequently purified by standard literature procedures[45,46] to yield [$N_{6,2,2,2}$][NTf_2] and [$P_{14,6,6,6}$][NTf_2], respectively. 1-Butyl-3-methylimidazolium tetrafluoroborate ([C_4mim][BF_4], high purity), 1-butyl-3-methylimidazolium hexafluorophosphate ([C_4-mim][PF_6], high purity), and 1-butyl-3-methylimidazolium trifluoromethylsulfonate ([C_4mim][OTf], high purity) were kindly donated by Merck KGaA. [C_4mim][BF_4] and [C_4mim]-[PF_6] were used as received. [C_4mim][OTf] was first diluted with CH_2Cl_2 and passed through a column consisting of alternating layers of neutral aluminum oxide and silica gel in order to remove residual acidic impurities. Bistrifluoromethane-

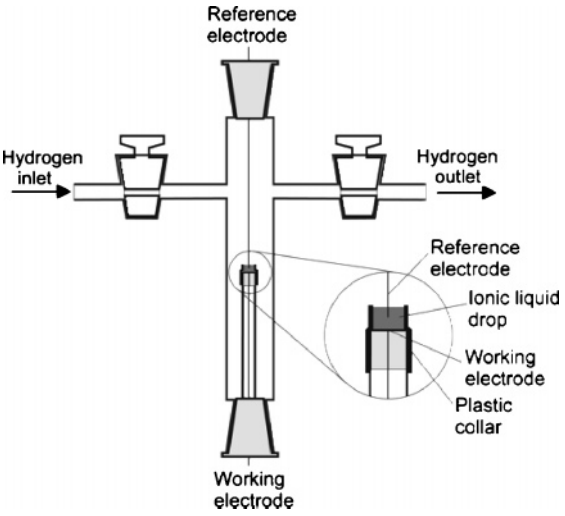

Figure 2. A cross section of the glass cell used to conduct electrochemical experiments on 20 μL samples of RTILs under conditions of controlled atmosphere

sulfonimide ($HNTf_2$, Fluka, >95%) was used as received and kept under an argon atmosphere during and after use. Ferrocene (Aldrich, 98%), tetrabutylammonium perchlorate (TBAP, Fluka, Puriss electrochemical grade, >99%), acetonitrile (Fischer Scientific, dried and distilled, >99.99%) were used as received without further purification. Hydrogen gas (99.995% pure) was purchased from BOC gases, Manchester, U.K.

2.2. Instrumentation. Electrochemical experiments were performed using a computer controlled μ-Autolab potentiostat (Eco-Chemie, Netherlands). A conventional two-electrode arrangement was employed, with a platinum electrode (10 μm diameter) as the working electrode and a 0.5 mm diameter silver wire as a quasi-reference electrode. The platinum microdisk electrode was polished on soft lapping pads (Kemet Ltd., U.K.) using alumina (Buehler, IL) of size 1.0 and 0.3 μm. The electrode diameter was calibrated electrochemically by analyzing the steady-state voltammetry of a 2 mM solution of ferrocene in acetonitrile containing 0.1 M TBAP, adopting a value for the diffusion coefficient of 2.3×10^{-5} cm^2 s^{-1} at 298 K.[47]

The electrodes were housed in a glass cell designed for investigating microsamples of ionic liquids under a controlled atmosphere, as shown in Figure 2. The working electrode was modified with a section of a disposable micropipette tip to create a small cavity above the disk into which a drop (~20 μL) of ionic liquid was placed. Prior to the addition of gas, the cell was purged using a vacuum pump (Edwards High Vacuum Pump, Model ES 50), which also served to remove impurities and trace atmospheric moisture naturally present in the IL. When the baseline showed little or no traces of impurities, hydrogen gas was introduced via one arm of the cell. The gas was then allowed to diffuse through the sample of the ionic liquid until equilibration was reached (typically after 10 min). Signals were monitored over a period of time to ensure that true equilibration was obtained. An outlet gas line led from the other arm of the cell into a fume cupboard.

For experiments involving the acid $HNTf_2$, stock solutions of approximately 130 mM were first made up in 1 mL of the corresponding $[NTf_2]^-$-based RTILs and were diluted to approximately 4 mM with a known amount of RTIL. Next, 20μL of this solution was pipetted into the plastic collar above the working electrode and then transferred into the T-cell and put under vacuum.

2.3. Chronoamperometric Experiments. Chronoamperometric transients for the reduction of $HNTf_2$ were achieved using a sample time of 0.1 s. The potential was held at 0 V for 20 s for pretreatment, after which the experimental transients were obtained, by stepping the potential to the required value and measuring the current for 10 s. Fitting of the experimental data was achieved using the nonlinear curve fitting function available in Origin 6.0 (Microcal Software Inc.), following the Shoup and Szabo approximation,[48] as employed by Evans et al.[49]

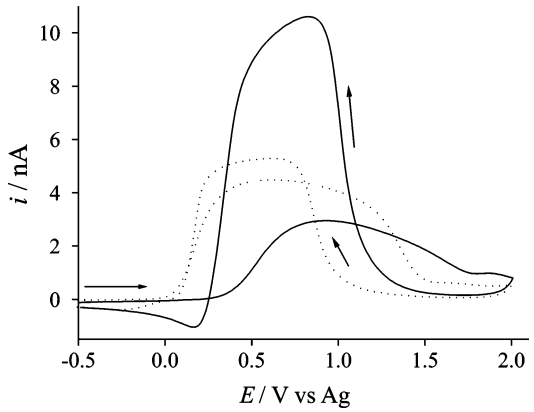

Figure 3. Cyclic voltammograms for the oxidation of 100% H_2 on a Pt electrode (diameter=10 μm) in the RTILs $[C_2mim][NTf_2]$ (solid line) and $[C_4mim][BF_4]$ (dotted line) with an anodic limit of 2.0V. Scan rate 100mVs^{-1}.

3. Results and Discussion

The oxidation of hydrogen, H_2, has been studied in a series of room-temperature ionic liquids (RTILs) on both gold and platinum microdisk electrodes of diameters of 10 and 25 μm. H_2 gas was allowed to diffuse through 20 μL of the liquid for at least 30 min in order to allow complete saturation, as evidenced by stable maximum peak currents. There were no noticeable oxidation peaks on either the 10 or 25 μm diameter gold electrodes, so we conclude that H_2 oxidation is voltammetrically inactive on gold. Sizable, reproducible peaks, however, were seen on both the 10 and 25 μm diameter platinum electrodes. All of the results presented below focus on the voltammetry obtained on the 10 μm diameter platinum electrode in a range of RTILs.

3.1. The Oxidation of Hydrogen on Platinum: Preliminary Observations. Figure 3 shows cyclic voltammograms obtained for the oxidation of H_2 on a platinum microdisk electrode (d = 10 μm) in the RTILs $[C_2mim][NTf_2]$ and $[C_4mim][BF_4]$ in the potential range −0.5 to 2.0 V vs Ag. The voltammetry shows a broad oxidation peak at approximately 0.9 and 0.5 V vs Ag for $[C_2mim][NTf_2]$ and $[C_4mim][BF_4]$, respectively. In $[C_2mim][NTf_2]$ (Figure 3 solid line), the peak decreases slowly until the potential reaches 1.8 V. When the scan is reversed at 2.0 V, the backward scan measures a lower current than the forward scan until 1.1 V, after which the current rapidly increases to a maximum at 0.9 V. The current then decreases rapidly at 0.5 V, showing a sharp cathodic peak at 0.2 V vs Ag. In $[C_4mim][BF_4]$, the anodic peak reaches a maximum at approximately 0.5 V, after which it slowly decreases to almost zero current. On reversal of the scan at 2.0 V vs Ag, the current on the backward scan is again less than on the forward scan. At 1.0 V, the current rises sharply to a maximum, after which it then decreases sharply at 0.1 V and shows the appearance of a small cathodic peak at −0.3 V vs Ag. The unusual form of wave shape has also been observed in the aprotic solvent DMSO by Barrette and Sawyer[32] using platinum macro-electrodes, although this phenomena was not fully investigated, and only forward voltammetric scans were shown.

The highly unusual shape of the voltammograms, in which the microelectrode current abruptly falls with increasing potential, might indicate that either (a) the voltammogram has passed through the potential of zero charge (PZC), giving rise to anions on the surface of the electrode rather than cations and hence a change in the electron-transfer kinetics, or (b) there is a point of transition where platinum oxides are formed at potentials positive of some threshold. We rule out (a), because the PZC for RTILs is thought to be much more negative than that observed in Figure 3. The PZC in $[C_4mim][BF_4]$ was reported[50,51] to be approximately -0.5 V vs Ag, and in $[C_n$-mim$][NTf_2]$ RTILs ($n = 8$, 10), the PZC was -0.254 and -0.161 V vs Ag/Ag^+, respectively. On the other hand, the formation of platinum oxides in the presence of hydrogen has been observed previously in aqueous solutions by Varela and Krischer[52] and was described by the following equations:

$$Pt + H_2O \rightarrow Pt{-}OH + H^+ + e^- \quad (3)$$

$$Pt{-}OH \rightarrow Pt{-}O + H^+ + e^- \quad (4)$$

It was suggested that Pt oxide formation sets in close to the upper turning point of the voltammogram, which leads to an inhibition of hydrogen oxidation, noted by the decrease in current and large hysteresis in the two scan directions. The formation of Pt oxide was also suggested briefly by Barette and Sawyer[32] for the oxidation of H_2 in aprotic solvents. Based on the shape of the voltammograms in Figure 3, it is likely that the same process is happening here. Equation 3 suggests that there must be a source of water present in order for platinum oxide formation, and we propose that a small amount of trace water present in the ionic liquid is enough to initiate such a reaction, noting that as little as monolayer oxide formation may be required to inhibit the H_2 oxidation reaction. We also note here that different RTILs will have different vapor pressures, leading to varying amounts of platinum oxide formation for each system. Although we have previously highlighted[9] that the experimental setup (employed in this work) is efficient in removing water from the RTIL, it is clearly not possible to obtain *completely* anhydrous IL samples.

The main difference between the voltammograms obtained in aqueous solvents and those presented in Figure 3 is noted: in aqueous solutions,[52] the current decreases rapidly after the formation of Pt oxide and remains close to zero on the reverse scan until the oxide is reduced. In all of the ionic liquids studied (with the exception of $[C_6mim]Cl$) the current on the reverse scan was *larger* than on the forward scan, resulting in a crossover of the scans and the appearance of a reduction peak at all scan rates studied (20 mV s^{-1} to 10 V s^{-1}).

On the second and subsequent scans in all RTILs, the forward peak current increases in comparison with the first scan, indicating that the electrode has been "activated" after scanning to 2 V. Varela and Krischer[52] report that the peak current on the second and subsequent scans in aqueous solutions remains similar, although the cathodic scans show behavior that suggests that, after an active/passive cycle is formed, the electrode reaches its highest activity that decreases with more cycles, until finally another active/passive cycle occurs. Repeat scans for unactivated electrodes were not discussed for the oxidation of H_2 in aprotic solvents.[32] Figure 4 shows the effect of activating the electrode in $[C_4mim][NTf_2]$ on a 10 μm diameter Pt electrode at a scan rate of 100 mV s^{-1}. The peak current of the anodic peak on the first cycle (bold solid line) is 3 nA, which increases to 11 nA on the reverse wide scan (dotted line). The peak current on the third scan (dot-dashed line) is 7 nA, more than twice that of the first scan. When the current is held for 1 min at 2.0 V vs Ag, the peak current on the next scan increased even further to 8 nA (dashed line). Holding the current for 5 min (thin solid line), however, did not increase the peak current to a higher value than holding for 1 min, indicating that the "activation" of the electrode is completed after 1 min.

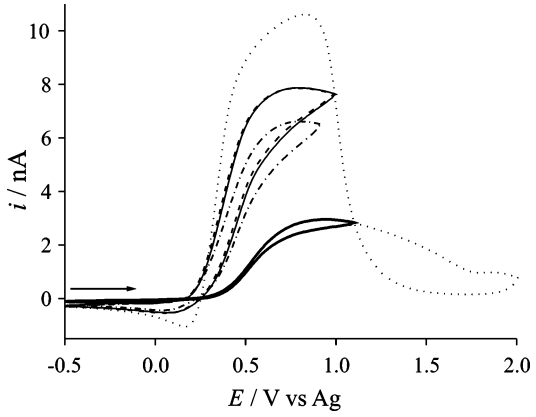

Figure 4. Cyclic voltammograms for the oxidation of 100% H_2 in $[C_4mim][NTf_2]$ on a 10 μm diameter Pt electrode, scan rate 100mVs^{-1}. Bold solid line=first scan, dotted line=second scan (with an extended anodic window), dot-dashed line=third scan, dashed line=scan taken after preanodization for 1 min, thin solid line=scan taken after preanodization for 5 min.

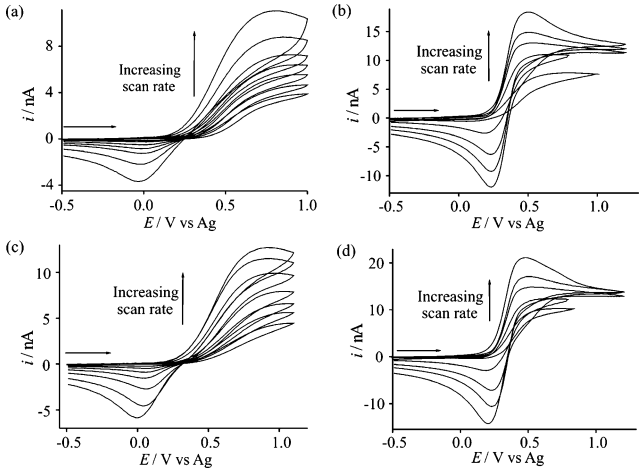

Figure 5. Cyclic voltammetry for the oxidation of 100% hydrogen on a 10 μm diameter Pt electrode in: (a) $[C_2mim][NTf_2]$ on a nonactivated electrode, (b) $[C_2mim][NTf_2]$ on an electrode activated for 1 min, (c) $[C_4mim][NTf_2]$ on a nonactivated electrode, and (d) $[C_4$-mim$][NTf_2]$ on an electrode activated for 1 min. Scan rates for activated electrodes are 0.1, 0.2, 0.4, 0.7, 1, 2 and 4 Vs^{-1}, and for nonactivated electrodes 0.1, 0.5, 1, 2 and 4 Vs^{-1}.

Deactivation of activated electrodes appears to occur over a number of minutes unless a second activating cycle is applied. Similar observations have been noted by Barrette and Sawyer[32] in the aprotic solvents MeCN, DMF, DMSO, and pyridine, whereas, in water, the activation lasted for 20 min, probably in each case due to the specific adsorption of trace impurities. It is expected that freshly reduced platinum oxide will give rise to a platinum surface that is free from adsorbed impurities when newly formed, until the adsorption of aprotic solvent molecules, which results in the deactivation of the electrode.[32]

3.2. The Oxidation of Hydrogen in $[NTf_2]^-$-Based RTILs: Activation vs Nonactivation. Figure 5 shows the oxidation of H_2 on a platinum microdisk electrode ($d = 10$ μm) in the RTILs $[C_2mim][NTf_2]$ (a and b) and $[C_4mim][NTf_2]$ (c and d). In both of these RTILs, voltammetry was obtained

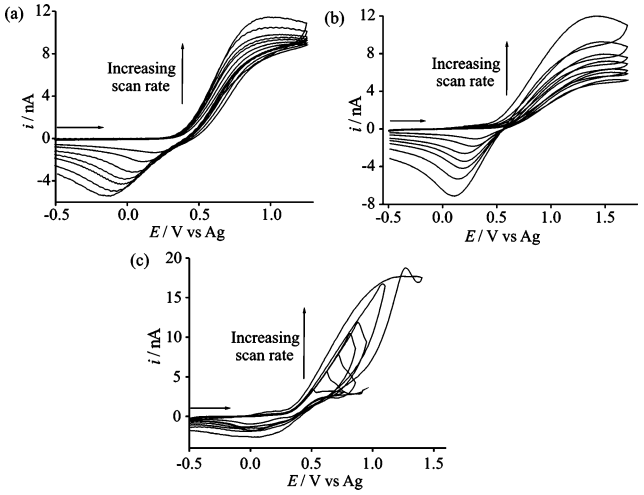

Figure 6. Cyclic voltammograms obtained for the oxidation of 100% H_2 in (a) $[N_{6222}][NTf_2]$ (b) $[P_{14666}][NTf_2]$ and (c) $[C_4mpyrr][NTf_2]$ on a Pt electrode ($d = 10$ μm) at scan rates of 0.1, 0.2, 0.4, 0.7, 1, 2 and 4 Vs^{-1}.

over a range of scan rates for both a "nonactivated" and "activated" electrode and appears to be diffusion controlled. In the case of the nonactivated electrode, the voltammetry obtained was relatively stable and reproducible, provided the solution was left to equilibrate for an appropriate amount of time between scans. In the aprotic solvents DMSO, DMF, pyridine, and MeCN, Barrette and Sawyer[32] report that the oxidation peaks of H_2 (prior to electrode activation) were broad and diffuse and that the peak currents were not reproducible and were not proportional to the partial pressure of H_2. For the oxidation of H_2 on both unactivated and activated electrodes, chronoamperometric transients showed severe adsorption effects and could not be fit to the Shoup and Szabo[48] expression.

The oxidation of H_2 was also studied in other $[NTf_2]^-$-based RTILs with cations other than the $[C_n mim]$ series. Figure 6 shows the oxidation of H_2 on a 10 μm diameter Pt electrode at a range of scan rates in (a) $[N_{6,2,2,2}][NTf_2]$, (b) $[P_{14,6,6,6}][NTf_2]$, and (c) $[C_4mpyrr][NTf_2]$. The voltammetry in the ammonium and phosphonium-based RTILs is similar to the imidazolium ($[C_n mim]$) RTILs, showing quasi-reversible behavior at all scan rates studied. However, the voltammetry in the pyrrolidinium RTIL (Figure 6c) is clearly different than all other $[NTf_2]^-$-based RTILs studied. Here, the onset of oxidation peaks are seen, but a sharp fall in the current is observed after the maximum. There is also no clear cathodic peak on the reverse scan, indicating that the product of the oxidation is unstable. It is suggested that the formation of platinum oxide occurs at potentials before that of the hydrogen oxidation in $[C_4mpyrr][NTf_2]$. This suggests that the structure of the cation is important in detecting the presence of dissolved hydrogen in RTILs, although action by impurities cannot be ruled out.

3.3. The Reduction of the Acid $HNTf_2$ in $[NTf_2]^-$-Based RTILs. The oxidation of H_2 in RTILs is presumed to lead to the formation of protons that are free to associate with the anions of the liquid. In the case of $[NTf_2]^-$-based RTILs, $HNTf_2$ (protonated form of $[NTf_2]^-$ in Figure 1) is likely formed. In order to try to fingerprint the corresponding reduction peak following the oxidation of hydrogen, the reduction of $HNTf_2$ was studied in both $[C_2mim][NTf_2]$ and $[C_4mim][NTf_2]$. Figure 7 shows the voltammetry obtained for the reduction of ca. 4 mM $HNTf_2$ over a range of scan rates on an unactivated Pt electrode ($d = 10$ μm) in the RTILs $[C_2mim][NTf_2]$ (7a) and $[C_4mim][NTf_2]$ (7b). In both RTILs, the wave appears to be

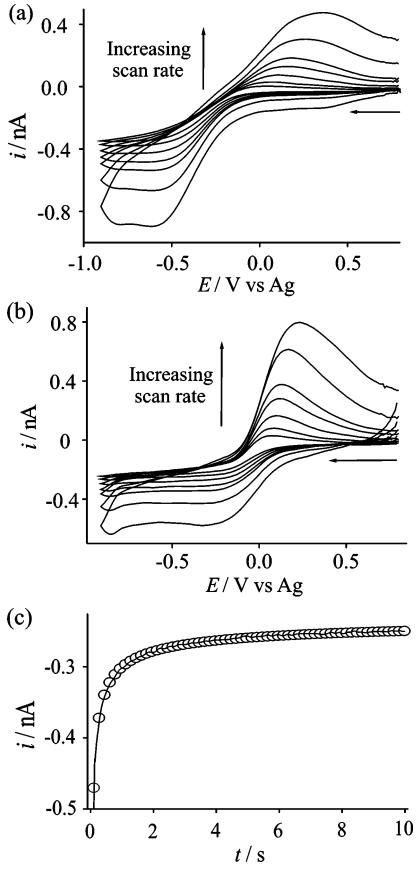

Figure 7. Cyclic voltammetry in (a) $[C_2mim][NTf_2]$ and (b) $[C_4mim][NTf_2]$ for the reduction of ca. 4 mM $HNTf_2$ on a Pt electrode (diameter=10 μm) at scan rates of 0.1, 0.2, 0.4, 0.7, 1, 2 and 4 Vs^{-1}. (c) Chronoamperometric transient obtained for the reduction of ca. 4 mM $HNTf_2$ on a Pt microdisk electrode ($d = 10$ μm), showing the experimental data (solid line) and fitted theoretical data (dots) following the Shoup and Szabo[48] expression.

electrochemically quasi-reversible (but not chemically irreversible) and the peaks appear to be relatively broad. The reduction of $HNTf_2$ in $[C_4mim][NTf_2]$ (7b) appears to be slightly more reversible than in $[C_2mim][NTf_2]$ (7a), as shown by the more defined anodic peak (7b).

In order to calculate diffusion coefficients and number of electrons transferred, a potential step was carried out on the reductive wave of the acid $HNTf_2$ in both $[C_2mim][NTf_2]$ and $[C_4mim][NTf_2]$. The potential was stepped from 0.0 V (corresponding to no faradaic current) to -0.75 V vs Ag in $[C_2mim][NTf_2]$ and to -0.55 V vs Ag in $[C_4mim][NTf_2]$, and the current was measured for 10 s (Figure 7a). The experimental data (solid line) was theoretically fit (dots) to the Shoup and Szabo[48] expression. The diffusion coefficient obtained for $HNTf_2$ in $[C_2mim][NTf_2]$ was calculated to be $(3.2 \pm 0.1) \times 10^{-11}$ m^2 s^{-1} and in $[C_4mim][NTf_2]$ was $(2.2 \pm 0.1) \times 10^{-11}$ m^2 s^{-1}, which seems reasonable considering the viscosities of $[C_2mim][NTf_2]$ (28 cP) compared to $[C_4mim][NTf_2]$ (44 cP), where the diffusion rates in the less viscous liquid are expected to be higher. The higher viscosity could also explain why the anodic peak appears to be larger in $[C_4mim][NTf_2]$ than in $[C_2mim][NTf_2]$: the slower diffusion of the species from the electrode surface in $[C_4mim][NTf_2]$ means that the product from the reduction stays close to the electrode surface for a longer time, resulting in a larger anodic peak. The results from chronoamperometric fitting also gave *nc* values (number of electrons $\times$ concentration) and indicated a one-electron process in both RTILs. This result also

implies for

$$HNTf_2 \rightleftharpoons H^+ + NTf_2^- \quad (5)$$

$$H^+ + e^- \rightarrow \frac{1}{2} H_2 \quad (6)$$

the pre-equilibrium is rapid, and $HNTf_2$ is fully reduced; otherwise, agreement with the Shoup and Szabo[48] expression would not be seen.

The reductive scan in Figure 7a, b at first sight suggests either a limiting current plateau characteristic of a diffusional controlled response at a microelectrode or the overlapping of two "cyclic voltammetric" peaks so as to give the illusion of a nearly constant current. Close inspection of Figure 7a, b hints at the latter, which is supported by the measurement of the diffusion coefficient for $HNTf_2$ alone. In particular, it is known[53] that, for steady-state voltammetry at a microelectrode, the following inequality must apply:

$$v \leq \frac{RTD}{nFr^2} \quad (7)$$

where v is the scan rate, R is the universal gas constant, T the absolute temperature, D is the diffusion coefficient, F the Faraday constant, and r the radius of the disk. For a scan rate of 4 V s^{-1}, as relative to the fastest scan reported in Figure 7, this inequality is strongly violated, confirming the likelihood that the observed voltammetry results from two overlapping peaks.

It is interesting to speculate how two peaks for the reduction of $HNTf_2$ might arise at a platinum electrode. In the case of proton reduction in aqueous media, the following general reaction scheme applies:

$$H^+ + e^- + M \xrightarrow{A} M - H \quad (8)$$

$$2M - H \xrightarrow{B} 2M + H_2 \quad (9)$$

$$M - H + H^+ + e^- \xrightarrow{C} H_2 + M \quad (10)$$

where M = the metal electrode surface. Depending on the identity of M, any of the transition states can be rate limiting; e.g., in the case of M═Pd, transition state B (eq 9) is the rate determining step (rds), whereas, for M═Hg, the rds is A (eq 8). In the case of M═Pt, the rds (in aqueous acid media) is C (eq 10), and this metal shows the fastest electrode kinetics in comparison with other metals.[54,55] In particular, the closeness of Pt to the apex of the volcano curve[54] relating the kinetics to the strength of the M−H bond suggests that the transition states A and C are not too dissimilar in energy, in the case of H^+ reduction in water. The currents flowing beyond the current maxima in Figure 7 are under diffusion control, as evidenced by the success of the chronoamperometric fitting. If the two inferred peaks are both due to hydrogen evolution from $HNTf_2$, it is possible that the second peak results from a slowing of the electrode kinetics of the $HNTf_2/H_2$ couple, perhaps resulting from the potential sweep passing through the PZC.

The occurrence or not of the two cathodic peaks appears to be sensitive to the parameters defining the sweep of the voltammogram, and under different potential sequences, either of the two peaks can be seen exclusively. Specifically when $HNTf_2$ is reduced with a voltammetric scan that begins at 0 V, two peaks are seen, which probably reflects a balance between the two of the three routes given in eqs 8−10. However, when the scan is swept from 1.0 V, only one reductive peak is seen, most likely corresponding to just one of the two routes and might explain why only one reductive peak is seen following the oxidation of hydrogen. The nature of the Pt surface including adsorbed species likely influences the role of the transition states A, B, and C, possibly via alteration of the PZC.

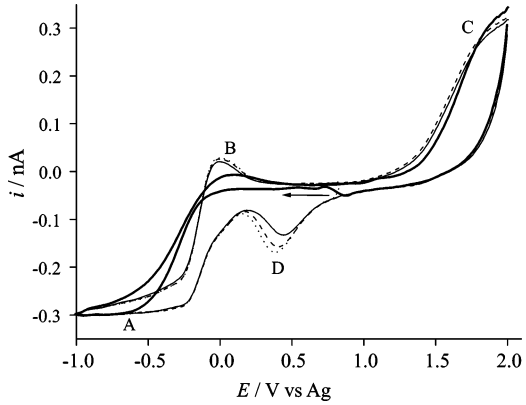

Figure 8. Cyclic voltammetry obtained for the reduction of ca. 4 mM $HNTf_2$ in [C_2mim][NTf_2] on a Pt electrode (diameter=10 μm) with an extended anodic limit of 2.0V. 4 scans are shown: first (bold solid), second (solid), third (dashed) and forth (dots), scan rate 0.1Vs^{-1}.

When comparing the voltammograms in Figure 7a, b to the voltammetry obtained for the oxidation of hydrogen on a nonactivated Pt electrode (Figure 5a, c) in the same RTILs, it is evident that the peak potentials do not overlay. However, the peak-to-peak separations are similar (approximately 0.86 and 0.91 V for the oxidation of H_2 and 0.92 and 0.85 V for the reduction of $HNTf_2$ in [C_2mim][NTf_2] and [C_4mim][NTf_2], respectively); the acid peaks are shifted by approximately −0.5 V from the hydrogen peaks. This likely reflects a shift in the quasi-reference electrode potential between the experiments. The potential is probably set up via the formation of silver oxides on the silver surface. Hydrogen is known to reduce oxides,[56] particularly thin films, so it is not surprising that such a shift in the voltammetry is observed. To show if this is the case, a further experiment was performed with 130 mM $HNTf_2$ and hydrogen gas both dissolved in the RTIL [C_2mim][NTf_2]. One reductive peak was observed when the scan was started at 0 V, whereas two peaks were observed when the scan was started at 1 V, which overlay almost exactly with the two peaks of $HNTf_2$ alone in [C_2mim][NTf_2] (Figure 7a). It is therefore suggested that the shift of 0.5 V between the H_2 peaks and $HNTf_2$ peaks is due to a shift in the reference potential.

Figure 8 shows the reduction of $HNTf_2$ at 100 mV s^{-1} on a platinum electrode (d = 10 μm) in [C_2mim][NTf_2] with an extended anodic limit of 2.0 V vs Ag. On the first scan, a relatively broad reduction peak, A, was seen, with a small anodic peak, B. When the anodic limit was extended, a further oxidation peak was seen, C, with a corresponding reduction peak, D. The charge under peak D was calculated to be 2.4×10^{-9} mol cm^{-2}, which gives a surface coverage of 1.45×10^{15} hydrogen atoms cm^{-2}, corresponding well to two reports[57,58] that give the number of hydrogen atoms in a monolayer as 1.5×10^{15} atoms cm^{-2} and 2×10^{-9} mol cm^{-2}, respectively. It is tentatively therefore thought that peak C, corresponding to the oxidation of $HNTf_2$, leads to the formation of products, the reduction of which leads to the formation of a monolayer of hydrogen atoms on the surface of the electrode. On the second and subsequent scans (solid, dashed, and dotted lines in Figure 8b), a sharper reduction peak was obtained for the acid, consistent with the "activating" effect that was seen for the hydrogen.

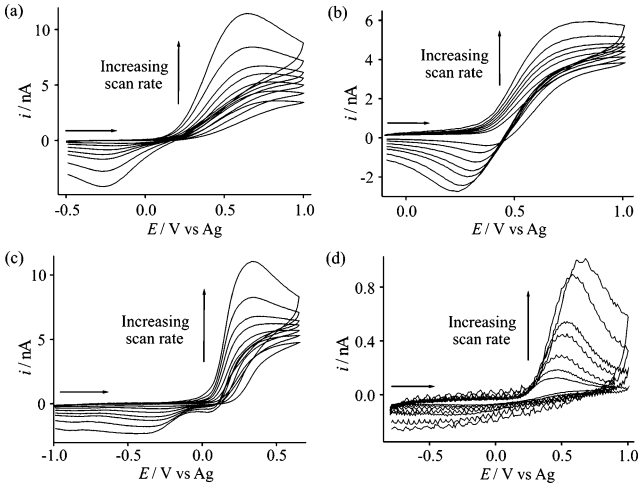

Figure 9. Cyclic voltammetry for the oxidation of 100% hydrogen on a nonactivated 10 μm diameter Pt electrode in: (a) [C_4mim][BF_4], (b) [C_4mim][OTf], (c) [C_4mim][PF_6] and (d) [C_6mim]Cl at scan rates of 0.1, 0.2, 0.4, 0.7, 1, 2 and 4 Vs^{-1}.

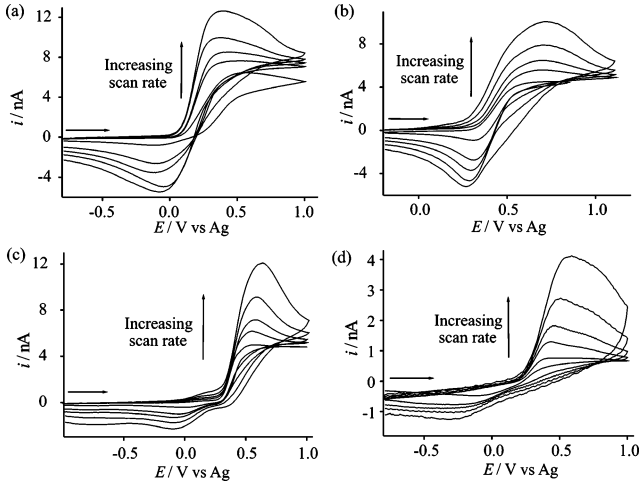

Figure 10. Cyclic voltammetry for the oxidation of 100% H_2 on a 10 μm diameter Pt electrode activated for 1 min in: (a) [C_4mim][BF_4], (b) [C_4mim][OTf], (c) [C_4mim][PF_6] and (d) [C_6mim]Cl at scan rates of 0.1, 0.5, 1, 2 and 4 Vs^{-1}.

3.4. The Oxidation of Hydrogen in RTILs with Different Anions: Activation vs Nonactivation. The effect of activation was also studied in ionic liquids with a common cation, [C_4mim]$^+$, and a range of different anions, namely [OTf]$^-$, [PF_6]$^-$, [BF_4]$^-$ and Cl^- (in [C_6mim]Cl). The voltammograms obtained over a range of scan rates for the oxidation of H_2 on a nonactivated platinum microdisk electrode (diameter = 10 μm) for these four RTILs are shown in Figure 9. In both [C_4mim][OTf] and [C_4mim][PF_6] (Figure 9a, b), partially reversible waves are observed, which indicates that the protons formed from the oxidation of H_2 react with the anions of these RTILs, and the product is stable-enough to be detected voltammetrically. HOTf and HPF_6 are both stable known molecules, so chemically reversible voltammetry is not unexpected. It is noted that the acid-catalyzed decomposition of [C_4mim][PF_6], has been previously reported by Swatloski et al.[59] They report the possible formation of the toxic product HF, and note the evolution of acidic HF fumes, and formation of a colorless solid around the reaction vessel containing the RTIL. The degradation of RTILs containing fluorine atoms is also briefly mentioned in a recent review paper.[60] Despite these findings, this process is not expected to feature heavily on the time scale of the experiment in [C_4mim][PF_6] such that quasi-reversibility is maintained.

For both [C_4mim][BF_4] and [C_6mim]Cl (Figures 9c and 9d), the voltammetric behavior is clearly different to the [NTf_2]$^-$ based RTILs, in that the reduction peak following the oxidation is much reduced in [C_4mim][BF_4], and is barely seen in [C_6mim]Cl. Little work has been reported concerning degradation of the [BF_4]$^-$ anion, despite various papers reporting this for [PF_6]$^-$.[59,60] Villagran et al.[61] appear to be the first to show that, in the presence of varying amounts of water, the decomposition of [C_4mim][BF_4] is much faster and more substantial than the decomposition of [C_4mim][PF_6]. It is predicted that for [C_4mim][BF_4], the product HBF_4 will dissociate according to the following (acid-catalyzed) equation:

$$HBF_4 \rightarrow HF + BF_3 \qquad (11)$$

The voltammograms shown in Figure 9b, c seem to agree well with these findings, and this should be to be taken into account when handling [BF_4]$^-$ based ionic liquids (particularly in the presence of proton sources) and applying them to green synthesis and indeed any application.

For [C_6mim]Cl, there are two possible products following the oxidation of hydrogen: (a) HCl or, we suggest more likely (b) [HCl_2]$^-$ (where H^+ is stabilized more in Cl^- media: see Introduction). Note that the voltammetry observed in [C_6mim]Cl (Figure 9d) appears to be relatively "noisy" due to the very small peak currents obtained because of the very high viscosity of this ionic liquid (7454cP at 293K). The voltammetry in [C_6mim]Cl seems to be further complicated by rapid reaction of the proton with the anion. This is assumed to correspond to the rapid formation of [HCl_2]$^-$, as previously postulated by Del Popolo et al.[42] for HCl in [C_1mim]Cl. The high viscosity also indicates that the product of the reaction will diffuse very slowly from the electrode surface, further suggesting [HCl_2]$^-$ (not HCl) as the reaction product based on the irreversibility of the system.

Figure 10 shows the voltammetry over a range of scan rates for the oxidation of hydrogen on an *activated* platinum electrode (d = 10 μm) in the RTILs [C_4mim][OTf], [C_4mim][PF_6], [C_4mim][BF_4] and [C_6mim]Cl. Here, the electrode was activated for 1 min at 2.0 V (1.6 V for [C_6mim]Cl due to the earlier solvent breakdown), and the scans were taken directly after. For three of the four RTILs, a small increase in peak current was seen after activation, whereas a 4-fold increase was observed in [C_6mim]Cl, making the signal-to-noise ratio much greater. For all four RTILs, Figure 10 shows that the peak has become slightly more reversible after activation, and the peak separations are smaller, in line with the results obtained [NTf_2]$^-$ based RTILs in Figure 5. The wave-shapes obtained in [C_4mim][OTf] and [C_4mim][PF_6] (Figures 10a and 10b) are now almost fully reversible, whereas the waves in [C_4mim][BF_4] and [C_6mim]Cl (Figures 10c and 10d) remain only partially reversible, confirming the instability of HBF_4 and HCl in these media.

4. Conclusions

The oxidation of hydrogen has been studied by cyclic voltammetry in a range of RTILs with different cations and anions. The appearance and position of the reverse (reduction) peak on the voltammograms is thought to depend on three factors: (1) the stability of the protonated anion, (2) the position of equilibrium of the protonation reaction (related to the pKa) and (3) any unusual follow-up chemistry, e.g., dissociation or reaction of the protonated anion. In particular, $HNTf_2$ is stable and easily reduced to H_2 so that the impression of quasi-electrochemically reversible kinetics is gained from voltammo-

grams such as that in Figure 5. Rather similar behavior is seen for $[OTf]^-$ based RTILs. On the other hand, the absence of a back-peak for $[C_6mim]Cl$ may indicate the formation of $[HCl_2]^-$. In the case of $[PF_6]^-$ and $[BF_4]^-$, intermediate characteristics are seen, perhaps indicating the scope for dissociation of the anion, especially for $[BF_4]^-$. This work has implications in both helping to define a pKa scale in RTILs, and for the amperometric sensing of H_2 gas.

References and Notes

(1) Earle, M. J.; Seddon, K. R., *Pure Appl. Chem.* **2000**, *72*, 1391.
(2) Marsh, K. N.; Deev, A.; Wu, A. C.-T.; Tran, E.; Klamt, A., Korean J. *Chem. Eng.* **2002**, *19*, 357.
(3) Wang, P.; Zakeeruddin, S. M.; Moser, J. E.; Graetzel, M. *J. Phys. Chem. B* **2003**, *107*, 13280.
(4) Buzzeo, M. C.; Hardacre, C.; Compton, R. G., *Anal. Chem.* **2006**, *76*, 4583.
(5) Ma, C. A.; Li, M. C.; Zheng, Y. F.; Liu, B. Y., *Electrochem. Solid-State Lett.* **2005**, *8*, 122.
(6) McEwen, A. B.; Ngo, H. L.; LeCompte, K.; Goldman, J. L., *J. Electrochem. Soc.* **1999**, *144*, L84.
(7) Howlett, P. C.; MacFarlane, D. R.; Hollenkamp, A. F., *Electrochem. Solid-State Lett.* **2004**, *7*, A97.
(8) Buzzeo, M. C.; Evans, R. G.; Compton, R. G., *ChemPhysChem* **2004**, *5*, 1106.
(9) Silvester, D. S.; Compton, R. G., *Z. Phys. Chem.* **2006**, *220*, 1247.
(10) Endres, F. *ChemPhysChem* **2002**, *3*, 144.
(11) Buzzeo, M. C.; Hardacre, C.; Compton, R. G., *ChemPhysChem* **2006**, *7*, 176.
(12) Evans, R. G.; Compton, R. G., *ChemPhysChem* **2006**, *7*, 488.
(13) Evans, R. G.; Klymenko, O. V.; Hardacre, C.; Seddon, K. R.; Compton, R. G., *J. Electroanal. Chem.* **2003**, *556*, 179.
(14) Evans, R. G.; Klymenko, O. V.; Price, P. D.; Davies, S. G.; Hardacre, C.; Compton, R. G., *ChemPhysChem* **2005**, *6*, 526.
(15) Evans, R. G.; Wain, A. J.; Hardacre, C.; Compton, R. G., *ChemPhysChem* **2005**, *6*, 1035.
(16) Silvester, D. S.; Wain, A. J.; Aldous, L.; Hardacre, C.; Compton, R. G., *J. Electroanal. Chem.* **2006**, *596*, 131.
(17) Fietkau, N.; Clegg, A. D.; Evans, R. G.; Villagran, C.; Hardacre, C.; Compton, R. G., *ChemPhysChem* **2006**, *7*, 1041.
(18) Lagrost, C.; Carrie, D.; Vaultier, M.; Hapiot, P., *J. Phys. Chem. A* **2003**, *107*, 745.
(19) Lagrost, C.; Preda, L.; Volanschi, E.; Hapiot, P., *J. Electroanal. Chem.* **2005**, *585*, 1.
(20) Silvester, D. S.; Aldous, L.; Lagunas, M. C.; Hardacre, C.; Compton, R. G., *J. Phys. Chem. B* **2006**, *110*, 22035.
(21) Amigues, E.; Hardacre, C.; Keane, G.; Migaud, M.; O'Neill, M., *Chem. Commun.* **2005**, *1*, 72.
(22) Jin, X.; Yu, L.; Garcia, D.; Ren, R. X.; Zeng, X., *Anal. Chem.* **2006**, 78.
(23) Pandey, S. *Anal. Chim. Acta* **2006**, *556*, 38.
(24) Buzzeo, M. C.; Klymenko, O. V.; Wadhawan, J. D.; Hardacre, C.; Seddon, K. R.; Compton, R. G. *J. Phys. Chem. B* **2004**, *108*, 3947.
(25) Buzzeo, M. C.; Giovanelli, D.; Lawrence, N. S.; Hardacre, C.; Seddon, K. R.; Compton, R. G., *Electroanalysis* **2004**, *16*, 888.
(26) Buzzeo, M. C.; Klymenko, O. V.; Wadhawan, J. D.; Hardacre, C.; Seddon, K. R.; Compton, R. G. *J. Phys. Chem. A* **2003**, *107*, 8872.
(27) O'Hayre, R.; Cha, S.-W.; Colella, W.; Prinz, F. B., *Fuel Cell Fundamentals*. John Wiley and Sons: New York, 2006; p 258.
(28) Belokopytov, V. P.; Aladzhalova, N. A., *Elektrokhimiya* **1966**, *2*, 1255.
(29) Jaworski, A.; Donten, M.; Stojek, Z.; Osteryoung, J. G., *Anal. Chem.* **1999**, *71*, 243.
(30) Will, F. G., *J. Electrochem. Soc.* **1963**, *110*, 145.
(31) Conway, B. E.; Novak, D. M., *J. Phys. Chem.* **1977**, *81*, 1459.
(32) Barrette, W. C.; Sawyer, D. T. *Anal. Chem.* **1984**, *56*, 653.
(33) Daniele, S.; Ugo, P.; Mazzocchin, G.-A. *Anal. Chim. Acta* **1985**, *173*, 141.
(34) Crowhurst, L.; Mawdsley, P. R.; Perez-Arlandis, J. M.; Salter, P. A.; Welton, T., *Phys. Chem. Chem. Phys.* **2003**, *5*, 2790.
(35) MacFarlane, D. R.; Forsyth, S. A. In *Ionic liquids as green solvents: progress and prospects*, *ACS Symp. Ser.* **2003**, *2003*; p 264.
(36) MacFarlane, D. R.; Pringle, J. M.; Johansson, K. M.; Forsyth, S. A.; Forsyth, M., *Chem. Commun.* **2006**, 1905.
(37) Thomazeau, C.; Olivier-Bourbigou, H.; Magna, L.; Luts, S.; Gilbert, B., *J. Am. Chem. Soc.* **2003**, *125*, 5264.
(38) Cole, A. C.; Jensen, J. L.; Ntai, I.; Tran, K. L. T.; Weaver, K. J.; Forbes, D. C.; Davis, J. H. J., *J. Amer. Chem. Soc.* **2002**, *124*, 5962.
(39) Du, Y.; Tian, F. *Synthetic Commun.* **2005**, *35*, 2703.
(40) Du, Z.; Li, Z.; Guo, S.; Zhang, J.; Zhu, L.; Deng, Y., *J. Phys. Chem. B* **2005**, *109*, 19542.
(41) Susan, M. A. B. H.; Noda, A.; Mitsushima, S.; Watanabe, M., *Chem. Commun.* **2003**, 938.
(42) Del Popolo, M. G.; Kohanoff, J.; Lynden-Bell, R. M., *J. Phys. Chem. B* **2006**, *110*, 8798.
(43) Earle, M. J.; Hakala, U.; Hardacre, C.; Karkkainen, J.; McAuley, B. J.; Rooney, D. W.; Seddon, K. R.; Thompson, J. M.; Wähälä, K., *Chem. Commun.* **2005**, 903.
(44) Hardacre, C.; Katdare, S. P.; Milroy, D.; Nancarrow, P.; Rooney, D. W.; Thompson, J. M., *J. Catal.* **2004**, *227*, 44.
(45) Bonhote, P.; Dias, A. P.; Papageorgiou, N.; Kalyanasundram, K.; Gratzel, M., *Inorg. Chem.* **1996**, *32*, 1168.
(46) MacFarlane, D. R.; Meakin, P.; Sun, J.; Amini, N.; Forsyth, M., *J. Phys. Chem. B* **1999**, *103*, 4164.
(47) Sharp, M. *Electrochimica Acta* **1983**, *28*, 301.
(48) Shoup, D.; Szabo, A. *J. Electroanal. Chem.* **1982**, *140*, 237.
(49) Evans, R. G.; Klymenko, O. V.; Saddoughi, S. A.; Hardacre, C.; Compton, R. G., *J. Phys. Chem.* B **2004**, *108*, 7878.
(50) Baldelli, S. *J. Phys. Chem. B* **2005**, *109*, 13049.
(51) Fitchett, B. D.; Rollins, J. B.; Conboy, J. C., *Langmuir* **2005**, *21*, 12179.
(52) Varela, H.; Krischer, K. *Catalysis Today* **2001**, *70*, 411.
(53) Bard, A. J.; Faulkner, L. R., *Electrochemical Methods: Fundamentals and Applications*. 2nd ed.; Wiley: New York, 2001.
(54) Reiger, P. H., *Electrochemistry*. 2nd ed.; Chapman and Hall, Inc.: New York, 1994; p 337.
(55) Trasatti, S. *J. Electroanal. Chem.* **1972**, *39*, 163.
(56) Fay, I. W.; Seeker, A. F., *J. Am. Chem. Soc.* **1903**, *25*, 641.
(57) Mostany, J.; Herrero, E.; Feliu, J. M.; Lipkowski, J., *J. Electroanal. Chem.* **2003**, *558*, 19.
(58) Treimer, S. E.; Evans, D. H., *J. Electroanal. Chem.* **1998**, *449*, 39.
(59) Swatloski, R. P.; Holbrey, J. D.; Rogers, R. D., *Green Chemistry* **2003**, *5*, 361.
(60) Xue, H.; Verma, R.; Shreeve, J. M., *J. Fluorine Chem.* **2006**, *127*, 159.
(61) Villagran, C.; Deetlefs, M.; Pitner, W. R.; Hardacre, C., *Anal. Chem.* **2004**, *76*, 2118.